Appl. Phys. B 70, 159–162 (2000) / Digital Object Identifier (DOI) 10.1007/s003409900105

Applied Physics B
Lasers
and Optics
© Springer-Verlag 2000

Diode-pumped $Ba(NO_3)_2$ and $NaBrO_3$ Raman lasers

J. Findeisen[1], H.J. Eichler[1], P. Peuser[2], A.A. Kaminskii[3], J. Hulliger[4]

[1] Optisches Institut, Technische Universität Berlin, Strasse des 17. Juni 135, D-10623 Berlin, Germany
(Fax: +49-30/3142-6888, E-mail: eichler@physik.tu-berlin.de)
[2] DaimlerChrysler AG, Forschung und Technik, Box 800465, D-81663 München, Germany
[3] Institute of Crystallography, Russian Academy of Sciences, Leninsky pr. 59, 117333 Moscow, Russia
[4] Dpt. of Chemistry and Biochemistry, University of Berne, Freiestr. 3, CH-3012 Berne, Switzerland

Received: 8 March 1999/Published online: 30 September 1999

Abstract. A Q-switched Nd:YAG laser transversely pumped with a 300-W quasi-cw diode generated pulses at 1.06 μm with intracavity energies of up to 10 mJ. Intracavity Raman shifting in a 60-mm-long $Ba(NO_3)_2$ crystal led to pulses with energies of 2.5 mJ at 1197 nm. The output pulse duration was reduced to 8.5 ns compared to 50 ns at the fundamental wavelength. Beam quality improvement was observed. A $NaBrO_3$ Raman laser generated pulse energies of 0.4 mJ at 1163 nm with a crystal of only 18 mm length. The Raman radiation was frequency doubled into the yellow spectral region from 580 nm to 599 nm, which is difficult to reach with other solid-state lasers.

PACS: 78.30; 42.55; 63.20

Frequency shifting of pico- and nanosecond laser pulses by stimulated Stokes and anti-Stokes Raman scattering (SRS) in crystals is of special importance, for example for ecological monitoring techniques [1].

Multiple wavelength cascades are generated covering wide spectral regions with $NaClO_3$. For example 16 different wavelengths between 1180 nm and 500 nm were measured [2].

$KGd(WO_4)_2$ and $Ba(NO_3)_2$ are well-known candidates for efficient stimulated Stokes Raman scattering to generate single wavelengths in the yellow spectral region [3–5] having phonon energies between 768 cm^{-1} for $KGd(WO_4)_2$ and 1047 cm^{-1} for $Ba(NO_3)_2$. Their spectroscopic and crystallographic properties have been investigated intensively [6–9]. $NaBrO_3$, a new Raman crystal, is of special interest as SRS active material, because of the strong Raman interaction with a vibrational mode with an energy of 795 cm^{-1} [10]. Intracavity SRS action can be achieved independently of the crystal axis due to the cubic symmetry in the case of $Ba(NO_3)_2$ and $NaBrO_3$.

In this work Raman pulses with conversion efficiencies up to 25% were obtained with $Ba(NO_3)_2$. Furthermore, in first experiments a conversion efficiency of 7% was achieved by using a relatively short $NaBrO_3$ crystal.

The Raman gain of $Ba(NO_3)_2$ reported in the literature to be $G_R \approx 11$ cm/GW at 1.06 μm wavelength is larger than in $KGd(WO_4)_2$ with $G_R \approx 7$ cm/GW and $PbWO_4$ with $G_R \approx 8.4$ cm/GW, which both were successfully used as Raman laser materials in SRS picosecond experiments performed by us [11]. This motivated the realization of a compact diode-pumped Q-switched Raman laser.

1 SRS action in $Ba(NO_3)_2$

Single-pass experiments without resonator mirrors were performed showing Stokes and conical anti-Stokes emission, which was analyzed by an OMA [3]. The polarized single pump pulses had an energy of 1 mJ and a pulse duration of 120 ps at 1.06 μm. The diameter of the focused pump radiation inside the crystal was 50 μm at the beam waist.

The intensity of the first Stokes line of $Ba(NO_3)_2$ at 1198 nm is suppressed, because of the sensitivity drop-off of the Si CCD-camera at wavelengths longer than 1100 nm. Six anti-Stokes lines extending to the visible were observed (Fig. 1).

Frequency-doubled ps-pulses at 532 nm generate strong Stokes Raman lines, which are also emitted in cones by Ra-

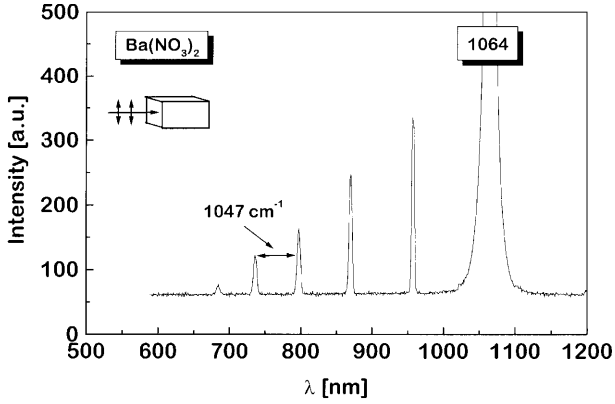

Fig. 1. Anti-Stokes SRS spectrum with 1064-nm pump wavelength

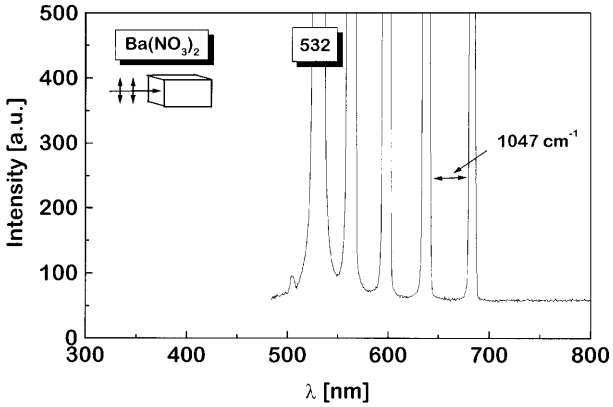

Fig. 2. Stokes SRS spectrum with 532-nm pump wavelength

man four-wave mixing (RFWM). The samples had a length of about 60 mm. In order to show in Figs. 1 and 2 the anti-Stokes emission as well, the intensity range was chosen small. Due to the CCD-sensitivity drop-off, the measured intensity of the anti-Stokes line in Fig. 2 is strongly reduced compared to anti-Stokes lines appearing up to the 6th order in Fig. 1.

$NaBrO_3$ showed seven anti-Stokes lines from the near infrared to the visible spectrum when pumped at 1.06 μm and five Stokes lines when pumped at 532 nm.

2 Diode-pumped Raman laser

The $Ba(NO_3)_2$ crystal was placed near the plane mirror inside a plane-concave resonator containing a side-pumped Nd:YAG crystal close to the curved mirror shown in Fig. 3.

On the rear side of the prism-shaped Nd:YAG crystal we placed a concave silver-coated HR mirror opposite the pump diode. This mirror with a focal distance of 2 cm was used to refocus the transmitted diode pump radiation back into the laser mode. For the experiments we used outcoupling mirrors having dielectric HR-coatings at 1064 nm with transmission values of 16% and 54% at 1198 nm. In the case of the 1163-nm line slightly more of the Stokes emission was coupled out with 59% transmission.

The curved end-mirror had a HR-coating extending from 1064 nm to 1200 nm, i.e. for all Stokes wavelengths resulting from phonon energies below 1050 cm^{-1}. A 300-W quasi-cw diode laser with three bars having a vertical extension of 0.8 mm and a horizontal extension of 10 mm was used for side-pumping the Nd:YAG crystal, which had a base length of 19 mm. Thus, the horizontal component of the emitted pump radiation was efficiently absorbed in the region of the laser mode. The distance between the diode bar and the AR-coated surface of the Nd:YAG crystal is less than 1 mm.

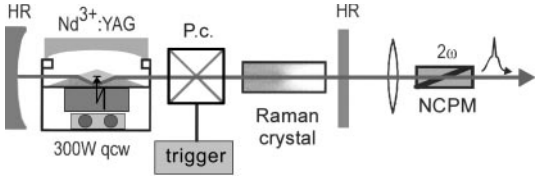

Fig. 3. Setup of the diode-pumped Q-switched Raman laser with the HR-coatings for the 1.06-μm pump radiation

The Nd:YAG crystal was cut with two Brewster faces for polarizing the laser light, which is a prerequisite for efficient SRS conversion.

Calculations of the laser mode led to a waist diameter of 580 μm at the outcoupling mirror and 820 μm inside the Nd:YAG crystal in case of TEM_{00} operation. This ensures a good overlap of the diode pump radiation emitted from the three bars with the 1.06-μm mode as well as sufficiently high SRS intensities.

By means of a Pockels cell Q-switching intracavity pulse energies of about 20 mJ were generated with lengths of 50 ns corresponding to intensities up to 80 MW/cm^2 inside the hygroscopic $Ba(NO_3)_2$ crystal placed in a sealed cell with Brewster endfaces assuming a beam diameter of about 700 μm as demonstrated in Fig. 4.

With this arrangement we obtained Raman pulse energies of 2.5 mJ as shown in Fig. 5.

The output energy corresponds to the amplification of a noise Stokes photon. The Raman gain can be estimated starting with the expression

$$G_R = \exp(g_R I_p(0) L n)\,, \qquad (1)$$

where $g_R \approx 11$ cm/GW is the small-signal Stokes gain coefficient, $I_p(0) = 80\,MW/cm^2$ is the Stokes intensity at the entrance into the Raman amplification medium, $L = 6$ cm is the length of the Raman medium. The cavity length of 30 cm

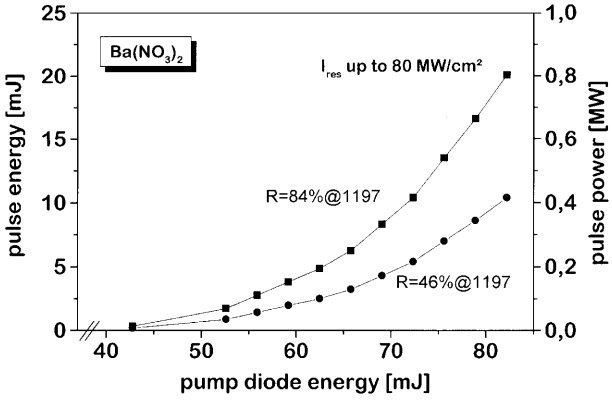

Fig. 4. Intracavity pulse energies of the Nd:YAG pump pulse in dependence of output coupling

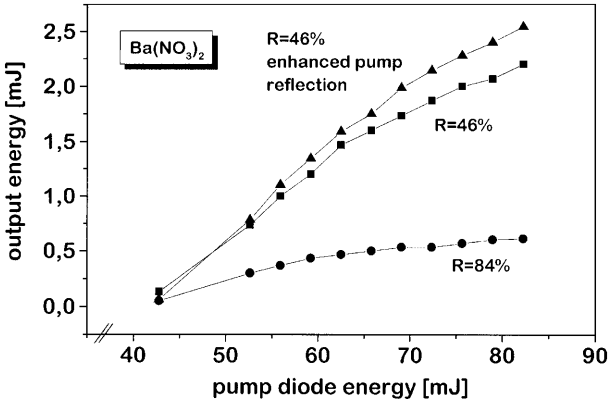

Fig. 5. Input and output energies of the $Ba(NO_3)_2$ Raman laser for two output coupling values

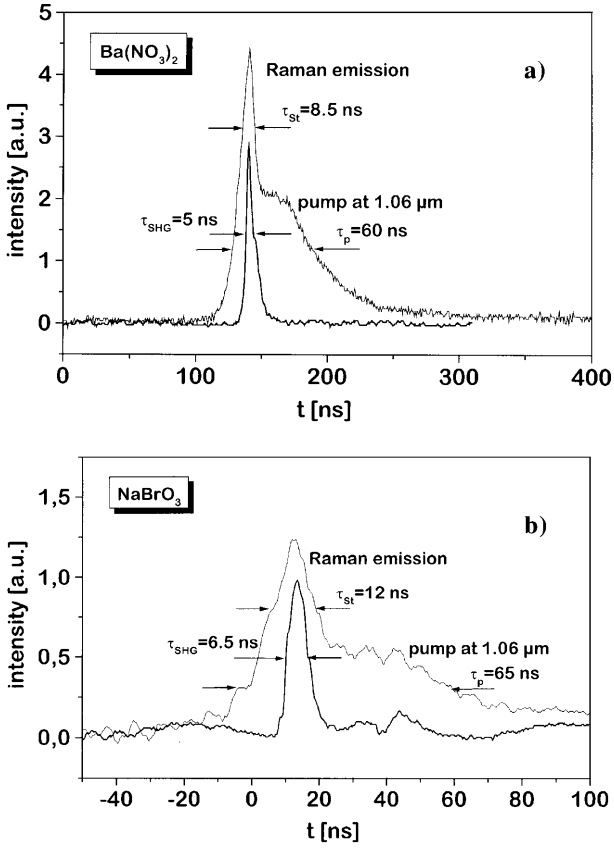

Fig. 6a,b. Temporal characteristics of pump-, Raman-, and frequency-doubled pulses for $Ba(NO_3)_2$ and $NaBrO_3$

leads to nine single passes (about 5 roundtrips) within the Stokes pulse length of approximately 9 ns. Taking an average value of $n = 9.5$ this yields $G_R = \exp(38) = 3.19 \times 10^{16}$, which means that a single photon with an energy of $h\nu = 1.68 \times 10^{-19}$ J at 1198 nm is amplified to $G_R h\nu \approx 5$ mJ output energy. This corresponds to the order of our experimental energy values.

3 Results and discussion

Figure 5 shows the output vs. input energy for two different reflectivities of the outcoupler for the Stokes radiation. It is obvious that the increase of the outcoupled Stokes pulse energy was obtained with the curved mirror on the rear side of the Nd:YAG crystal for refocusing the diode pump radiation back into the laser crystal.

With this arrangement we obtained Raman pulse energies of 2.5 mJ as shown in Fig. 5. The average Raman output power at 1197 nm shows a linear dependence on the repetition rate. The maximum power was about 107 mW at 47-Hz operation limited by the diode driver. Conversion to 599 nm was performed in LBO by noncritical phase matching (NCPM) at 28 °C. The SHG pulse energy achieved with $Ba(NO_3)_2$ is $E = 0.6$ mJ with a peak power of 0.12 MW at 5 ns pulse duration. The average power amounts to 21 mW at 47 Hz.

The $NaBrO_3$ Stokes emission was converted to 581 nm at 51 °C NCPM temperature. An energy of 0.4 mJ was measured for the Stokes pulses and of 0.15 mJ for the frequency-doubled yellow radiation. The average output powers were 18 mW and 6.5 mW, respectively. This crystal is hygroscopic

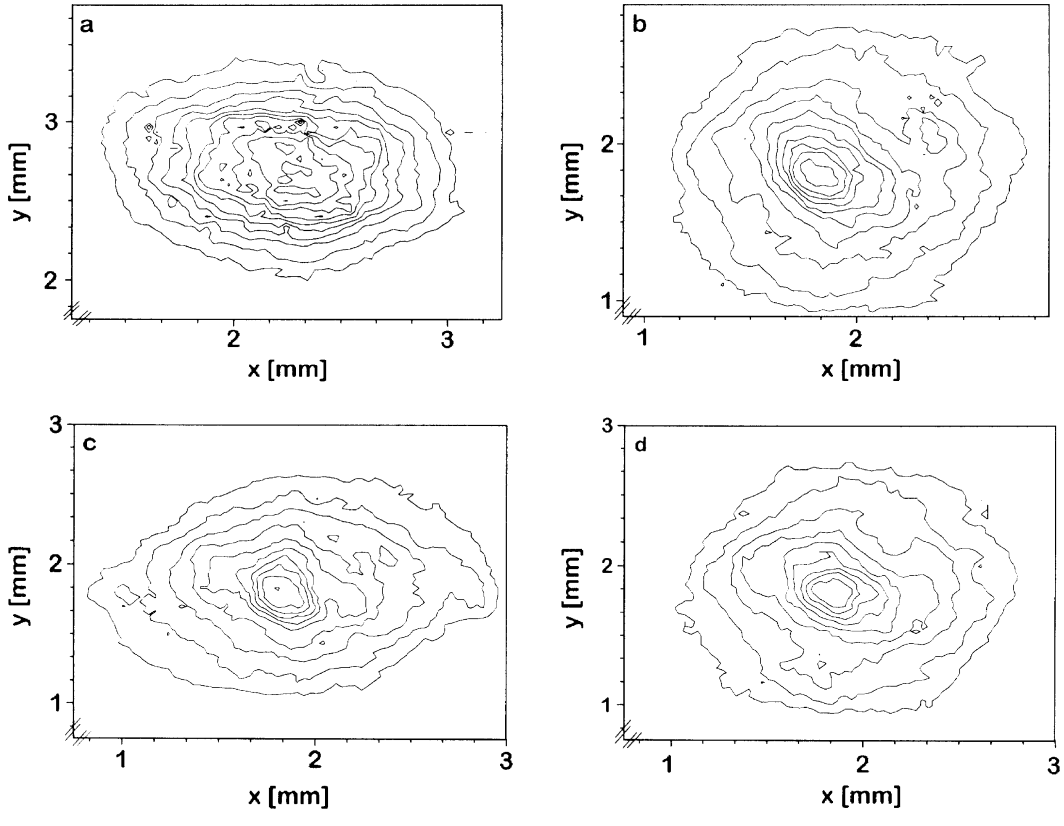

Fig. 7a–d. Contour plots of the pump- (**a**) and Raman laser (**b**) modes without transverse mode control (**a**, **b**) and with mode aperture (**c**, **d**)

Table 1. Phonon energy E_{ph}, Raman gain G_R [4, 5], bandwidth $\Delta\nu_R$, dephasing time T_2, threshold energy E_{thr}, output energy E_{out}, conversion efficiency ε, and SHG energy E_{SHG}

Crystal	E_{ph}/ cm^{-1}	G_R/ cm/GW	$\Delta\nu_R$ (cm^{-1})/ $\Delta\nu_R$(GHz)	T_2/ps	E_{thr}/mJ (Pump)	I_{max}/ MW/cm^{-2}	E_{out}/mJ (1^{st} Stokes)	Conversion Eff. ε/%	E_{SHG}/ mJ
$Ba(NO_3)_2$	1047	≈ 11	0.6/0.2	≈ 9	1	60	2.5	25	≈ 0.6
$NaBrO_3$	795	–	–	–	5	22	0.4	7	≈ 0.15

as well and was yet not placed into a sealed cell. Degradations of the plane parallel polished surface were already visible.

The reduction of pulse duration by SRS is demonstrated in Fig. 6. The Raman pulse starts when the pump pulse power exceeds the SRS threshold. The Raman pulse of $\tau_{St} = 8.5$ ns is about six times shorter than the pump pulse of $\tau_p = 50$ ns measured without SRS. The pump pulse had a duration of $\tau_p = 60$ ns because of the smaller gain of the 1.06-μm emission during SRS generation and outcoupling. The width of the SHG pulse was shortened to $\tau_{SHG} = 5$ ns.

In the case of $NaBrO_3$ a similar behaviour is observed. The pump pulse of 55 ns was shortened to a Raman pulse duration of 12 ns. The yellow SHG pulse had a duration of 6.5 ns. A small part of the 1.06-μm pump radiation transmits through the outcoupler and is detected by the photodiode as well, forming the pedestal of the Raman pulse.

As can be seen from Fig. 7a,b the elliptical pump mode was transformed into a nearly spherical Raman mode indicating a beam clean-up effect in $Ba(NO_3)_2$.

Fundamental mode operation was obtained also by placing an aperture of 0.8 mm into the resonator in order to achieve a good match to the Raman mode. In this case a significant beam clean-up was not observed (Fig. 7c,d). This demonstrates that a higher output energy is generated without any aperture for transverse mode control. Results of ns Raman laser experiments with $Ba(NO_3)_2$ and $NaBrO_3$ are summarized in Table 1.

4 Conclusions

Efficient intracavity Raman conversion was demonstrated for nanosecond pulses in a compact diode-pumped Nd:YAG laser. Unlike birefringent Raman active crystals which have to be acousto-optically Q-switched, the cubic crystal symmetry of $Ba(NO_3)_2$ and $NaBrO_3$ allows the use of a standard Pockels cell for Q-switching.

First results of the Raman laser action with a near-plane-parallel cubic $NaBrO_3$ sample of only 18 mm length, which had uncoated endfaces, showed that this crystal is a promising candidate for Raman lasers. Longer $NaBrO_3$ crystals with AR-coated and plane-parallel endfaces placed in sealed cells due to their hygroscopic properties will extend the wavelength range in the visible spectral region, which can be covered by efficient all-solid-state Raman shifters.

Acknowledgements. This work was supported by DFG/RFFI (grant 436 RUS 17/95/98 (R)). One of us (J.F.) acknowledges also partial support from the "Acciones Integradas" programme of the DAAD. The authors achnowledge that the investigation had considerable assistance from the joint open Laboratory for Laser Crystals and Precise Laser Systems, where P. Franz performed the growth experiments for the $NaBrO_3$ crystals.

References

1. J.T. Murray, W. Austin, R.C. Powell, G.J. Quarles: In *Advanced Solid State Lasers*, Orlando, 1997, Technical Digest (Optical Society of America, Washington, DC 1997) pp. 11–13
2. A.A. Kaminskii, J. Hulliger, H.J. Eichler, J. Findeisen, A.V. Butashin, R. Macdonald, S.N. Bagayev: Appl. Phys. B **67**, 157 (1998)
3. J. Findeisen, H.J. Eichler, A.A. Kaminskii: IEEE J. Quantum Electron. **QE-35**, 173 (1999)
4. C. He, T.H. Chyba: Opt. Commun. **135**, 273 (1997)
5. K.A. Stankov, G. Marowsky: Appl. Phys. B **61**, 213 (1995)
6. S.V. Borisov, R.F. Kletsova: Kristallografiya **13**, 517 (1968)
7. M.C. Pujol, M. Rico, C. Zaido, R. Solé, V. Nikolov, X. Solans, M. Aguiló, F. Díaz: Appl. Phys. B **68**, 187 (1999)
8. T.T. Basiev, A.A. Sobol, P.G. Zverev, Yu.K. Voronko, V.V. Osiko, R.C. Powell: In *Advanced Solid State Lasers*, Coeur d'Alene, 1998, Technical Digest (Optical Society of America, Washington, DC 1998) pp. 24–25
9. P.G. Zverev, T.T. Basiev, V.V. Osiko, A.M. Kulkov, V.N. Voitsekhovskii, V.E. Yakobson: Opt. Mater. **11**, 315 (1999)
10. P. Franz, P. Egger, J. Hulliger, J. Findeisen, A.A. Kaminskii, H.J. Eichler: Phys. Status Solidi B **210**, R7 (1998)
11. A.A. Kaminskii, H.J. Eichler, K. Ueda, N.V. Klassen, B.S. Redkin, L.E. Li, D. Jaque, J. Findeisen, J. García-Solé J. Fernandez, R. Balda: Appl. Opt. **38**, 4533 (1999)